Kinetics, acid sites and deactivation of H-mordenite during the SCR of NO_x with CH_4

A. Ribotta, M. Lezcano, M. Kurgansky, E. Miró, E. Lombardo and J. Petunchi

Instituto de Investigaciones en Catálisis y Petroquímica – INCAPE (FIQ, UNL-CONICET), Santiago del Estero 2829, 3000 Santa Fe, Argentina
E-mail: nfisico@fiqus.unl.edu.ar

C. Moreaux and J.M. Dereppe

Laboratoire de Chimie-Physique, Université Catholique de Louvain, PJ L. Pasteur 1Bte 3D, 1348 Louvain-la-Neuve, Belgium

Received 25 May 1997; accepted 19 September 1997

H-mordenites are active for the SCR reaction but they suffer irreversible partial deactivation after being on stream for one hour at 650°C. The reaction orders and activation energies are not significantly affected by deactivation. This indicates that deactivation originates in a decrease in the number of active sites due to dealumination and possible pore blockage. The NO disappearance rate correlates with TPD NH_3 between 300 and 700°C; FTIR confirms these results. ^{129}Xe NMR of adsorbed xenon shows that pore blockage occurs and is due to the presence of aluminum species in the main zeolite channels. The overall deactivation process and the role of acid sites is discussed in terms of the current literature.

Keywords: SCR of NO with CH_4, H-mordenite, deactivation, acid sites, kinetic parameters

1. Introduction

The use of CH_4 as a substitute for NH_3 in the removal of nitrogen oxides from oxygen-rich streams has become of particular interest. Since Li and Armor [1] reported that Co-ZSM5 is an effective catalyst for this reaction, a great variety of materials have been studied [2–4] with the same purpose.

Ga,H-ZSM5 [5] and Pd,H-ZSM5 [6,7] have been reported as effective catalysts, the former being more reactive and selective than Co-ZSM5 [2] under a dry atmosphere over 500°C. Unfortunately, the gallium loaded zeolites are much more sensitive to water. For both catalysts, Ga,H- and Pd,H-ZSM5, the authors claimed that acid sites play a central role in the reduction of NO. In the same vein, Yogo et al. [8] found that H-zeolites were active and selective for the NO reduction with CH_4 in an oxygen-rich atmosphere. They investigated H-ZSM5, H-ferrierite and H-mordenite and pointed out that the amount of acid sites is the essential factor for the reaction.

Loughram and Resasco [7], in their studies of the SCR of NO_x by methane over palladium on several acidic and non-acidic supports, found that the H-ZSM5 support was not unique in promoting the activity of palladium but that other acidic supports such as sulfated zirconia also exhibited promoting effects. Kintaichi et al. [9], Hamada et al. [10] and Satsuma et al. [11], using different hydrocarbons as NO_x reducing agents in excess oxygen over several catalysts, also claimed a dependence of the catalytic behavior on the acidic properties of the solids.

Hall and co-workers [12,13] also found that H-ZSM5 is an effective catalyst for the NO_x reduction with CH_4. However, they claimed that it is unnecessary to assume that acid catalysis plays a role in the selective catalytic reduction of NO_x [12]. On the other hand, the presence of protons in zeolites makes them more susceptible to on-stream dealumination, as has been well documented by several authors [14–16].

The present work is aimed at better defining both the deactivation phenomena occurring on H-mordenite as reported elsewhere [17] during the SCR of NO_x with CH_4, and the role, if any, of the acid properties of the solids in the reaction as well as how they relate to deactivation. To attain this goal, we performed FTIR and NH_3 TPD studies on a series of H-mordenites with various Si/Al ratios before and after the SCR of NO_x with CH_4 at high temperature. With the same purpose, we compared the kinetic behavior of the fresh samples with the one obtained with deactivated samples and performed additional studies on the ^{129}Xe NMR of physisorbed xenon.

2. Experimental

2.1. Catalysts preparation and characterization

A commercial H-mordenite (Norton Zeolon 900 H)

with a $(Si/Al)_{Ch}$ ratio of 5.9 (MH5.9), determined by chemical analysis, was the starting material. The dealumination was performed with HNO_3 at 90°C under the following conditions: 2, 7 and 24 h with HNO_3 concentration of 4 and 14 N, respectively.

The samples obtained are named: MH7.3, MH11.0, and MH16.9 with unit cell compositions: $H_{5.8}[(AlO_2)_{5.8}(SiO_2)_{42.2}]$, $H_{4.0}[(AlO_2)_{4.0}(SiO_2)_{44}]$ and $H_{2.7}[(AlO_2)_{2.7}(SiO_2)_{45.3}]$, respectively, from chemical analysis.

Before the kinetic experiments, the solids were pretreated as follows: 1.5 h at 110°C, 2 h at 210°C and 8 h at 400°C (heating rate: 2°C/min in all cases). The pretreatment was carried out under vacuum for gas adsorption and infrared experiments, in flowing dry He for ammonia TPD and in flowing dry oxygen for catalytic tests. This procedure is called herein "standard pretreatment".

2.2. ^{129}Xe NMR of physisorbed xenon

After the standard pretreatment, xenon was adsorbed at 20°C in a conventional BET system which allowed the measurement of the amount of physisorbed Xe at different equilibrium pressures.

Spectra were taken at a frequency of 82.91 mHz using a MSL 300 Bruker Spectrometer. Between 1000 and 5000 scans were performed in order to obtain a good signal/noise ratio. The chemical shift was measured between 10 and 600 mbar of Xe pressure and referred to the NMR signal of Xe in the gas phase extrapolated at zero pressure.

2.3. Ammonia TPD

NH_3 was adsorbed at 100°C till the saturation of the sample was achieved. It was kept at 100°C for 4 h in He stream. The TPD was conducted with a heating rate of 10°C/min between 100 and 700°C. The solid was maintained at 700°C until recovering the base line.

2.4. Infrared spectra

Infrared spectra were recorded using an FTIR Shimadzu DR-8001 instrument collecting 2000 spectra with spectral resolution of 4 cm^{-1}. Self-supporting wafers of the samples (7–10 mg/cm^2) were mounted on a transportable infrared cell fitted with KBr optical windows. The measurements were made under vacuum at room temperature after the standard pretreatment.

2.5. Cataytic experiments

Steady-state kinetic experiments were performed using a single-pass flow reactor made of fused silica with an inside diameter of 5 mm and 300 mm long, operating at atmospheric pressure. The reacting mixture was obtained by mixing four gas lines independently controlled with mass flow controllers. The details of this apparatus are given elsewhere [17].

For the kinetic measurements, temperature ranged between 450 and 550°C, CH_4 and NO concentrations were varied from 400 to 2000 ppm, and oxygen from 0 to 10%. GHSV varied between 6,000 and 60,000 h^{-1}. In the experiments performed with H_2O vapor, the He flow passed through a water saturator so as to obtain a 2% concentration in H_2O. The gas blends were analyzed before and after reaction using a Varian 3700 G.C. instrument. Zeolite 5A was used to separate N_2, O_2, NO, CO and CH_4 and Chromosorb 102 to analyze CO_2, C_2H_4 and N_2O.

The conversions for the selective reduction were calculated in terms of N_2 production as $C_{NO} = 2[N_2]/[NO]$, and for CH_4 as $C_{CH_4} = [CO_x]/[CH_4]$, where $[N_2]$, $[CO_x]$ are gas phase concentrations after reaction and [NO], $[CH_4]$ are feed concentrations. The carbon balance was always better than 95% and the conversions reported were determined after the steady state was reached (usually after 1 h on stream).

The rates of NO reduction and total methane oxidation were determined under differential conditions (conversions lower than 10%) using the expression:

$$R_G(\text{mol}/(\text{h g})) = F_G \times C_G/W \times 100\,, \qquad (1)$$

where F_G is the gas molar flow of G (mol/h), C_G the conversion of G, and W the catalyst weight (g). To check the validity of the parameters obtained under differential conditions, the operation of the integral reactor was simulated. For this purpose the equations given below were integrated using numerical methods:

$$d[NO]/dt = -k_1[NO]^a[CH_4]^b[O_2]^c\,, \qquad (2)$$

$$d[CH_4]/dt = -k_2[NO]^d[CH_4]^e[O_2]^f\,, \qquad (3)$$

where the concentrations of the reactants in mol/cm^3 are between brackets, t is the residence time in the reactor ($t = W/F$), and $k_1, k_2, a, b, c, d, e, f$, are the empirical kinetic parameters calculated from data obtained under differential conditions.

3. Results and discussion

3.1. Catalytic behavior

The catalytic results shown in figure 1 and table 1 for mordenites with different Si/Al ratios confirm what was previously reported [17], i.e., that the NO to N_2 conversion is a function of the framework Si/Al ratio in protonic mordenites and that these materials are irreversibly deactivated after being on stream at 650°C. In order to analyze the effect of the reaction time on deactivation, long-term experiments at constant temperature were

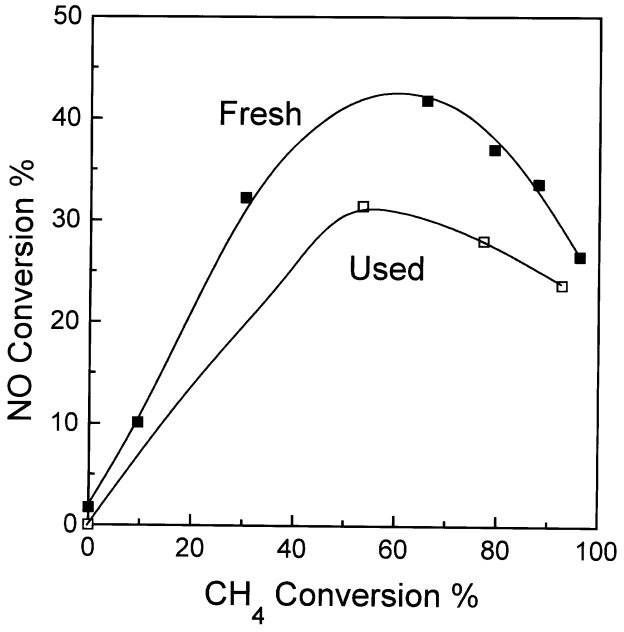

Figure 1. Effect of high reaction temperature on selectivity of MH5.9. (■) Fresh sample. (□) After 1 h on stream at 650°C (used sample). Reaction conditions: GHSV: 6500 h^{-1}, temperature range: 300–650°C, NO: 1000 ppm, CH_4: 1000 ppm, O_2: 10%.

performed. It was observed that up to 550°C the samples were stable for at least 27 h on stream. Figure 2 shows the behavior observed for the case of the fresh MH5.9 catalyst.

Under real reaction conditions, the catalysts are exposed to an atmosphere with water vapor generated during combustion. Consequently, it is important to know the effect of H_2O added in the feed stream. Figure 3 shows the results obtained in the presence of added H_2O. Note that an important drop in the NO_x and CH_4 conversions occurred. When water is eliminated from the feed, the activity is rapidly recovered.

3.2. NH_3 TPD and FTIR characterization

In order to attain a better understanding of the deactivation phenomena and, consequently, of the characteristics of the active sites for the reaction under study, NH_3 TPD and FTIR experiments were carried out to investigate the acidic properties of the solids employed and how they could be affected by the reaction conditions. Figures 4A and 4B show the NH_3 desorption thermograms of the fresh and used samples. The traces obtained are in agreement with those reported by other authors for H-mordenites [18]. The peaks at low temperature are due to physisorbed or weakly chemisorbed NH_3 and, hence, they do not represent acid sites (compare with the Na-mordenite sample). The temperature maxima in the 550–600°C range are practically independent from the Si/Al ratio; this would indicate a similar acid strength distribution for all the samples. Nevertheless, due to the width of these peaks no clear discrimination of any possible difference can be obtained.

For quantitative purposes, the amount of desorbed NH_3 at temperatures higher than 300°C may be calculated using different procedures. In a previous paper [19] we calculated the concentration of strong acid sites from the amount of NH_3 desorbed between 300 and 700°C. On the other hand, Meyers et al. [18] found that there is a tail of the low temperature peak and used this "tail" as the "baseline" for the high temperature desorption. We have now adopted this procedure and found that the calculated amount of NH_3 more closely conforms to the expected $NH_3/Al^{IV} = 1$ ratio in the fresh samples (table 1 and figure 5). The NH_3 TPD profiles of the used samples (figure 4B) show an important effect of the reaction conditions (results obtained after

Table 1
Effect of framework on NH_3 temperature-programmed desorption

Catalyst	Al^{IV} [a] (g) $\times 10^{21}$	Al^{tot} [b] (g) $\times 10^{21}$	T_{max} [c] (°C)		$NH_3$2P [d] (g) $\times 10^{21}$	NH_3T [e] (g) $\times 10^{21}$	C_{NO} [f] (%)	C_{CH_4} [g] (%)
			1st peak	2nd peak				
MHF5.9	0.55	1.42	176	520	0.64	1.1	41.8	70
MHU5.9	0.39	1.42	200	n/d	0.19	1.1	31.4	50
MHF7.3	0.49	1.19	176	520	0.40	0.97	26.3	65
MHU7.3	0.31	1.19	176	440	0.11	0.97	18	65
MHF11.0	0.31	0.83	176	520	0.38	0.86	24.3	50
MHU11.0	0.20	0.83	176	415	0.09	0.72	14	40
MHF16.9	0.23	0.57	176	568	0.34	0.61	15	30
MHU16.9	0.18	0.57	176	n/d	0.10	0.53	4.9	25

[a] Framework Al, obtained by measuring only the intensity of the 54 ppm signal corresponding to Al^{IV} referred to Valfor CP 500 (see ref. [17]).
[b] Al content from chemical analysis.
[c] Temperature at peak minima (estimated) n/d not-defined.
[d] Molecules of NH_3 desorbed at temperatures higher than 300°C.
[e] Total NH_3 molecules desorbed.
[f] Maximum conversion of NO to N_2 (500–550°C temperature range).
[g] Maximum conversion of CH_4 at maximum C_{NO} (500–550°C temperature range).

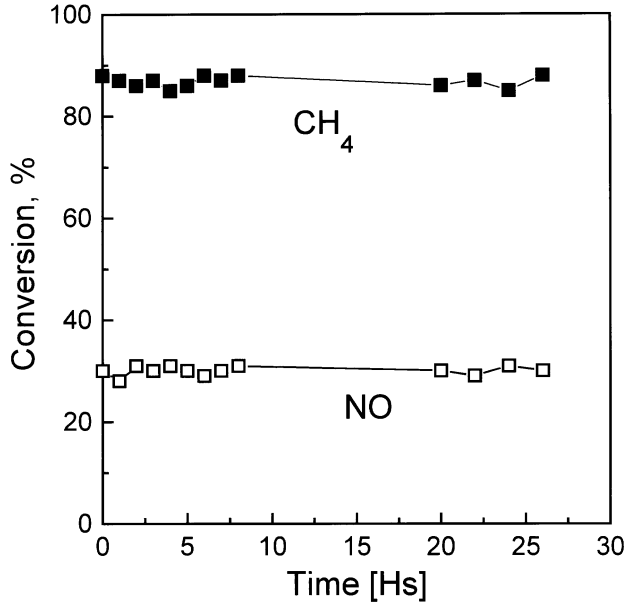

Figure 2. H-mordenite stability at 550°C for MH5.9. (□) NO to N_2 conversion and (■) CH_4 to CO_2 conversion. Reaction conditions: GHSV: 6500 h^{-1}, *T*: 550°C, NO: 1000 ppm, CH_4: 1000 ppm, O_2: 10%, the balance to one atmosphere with He.

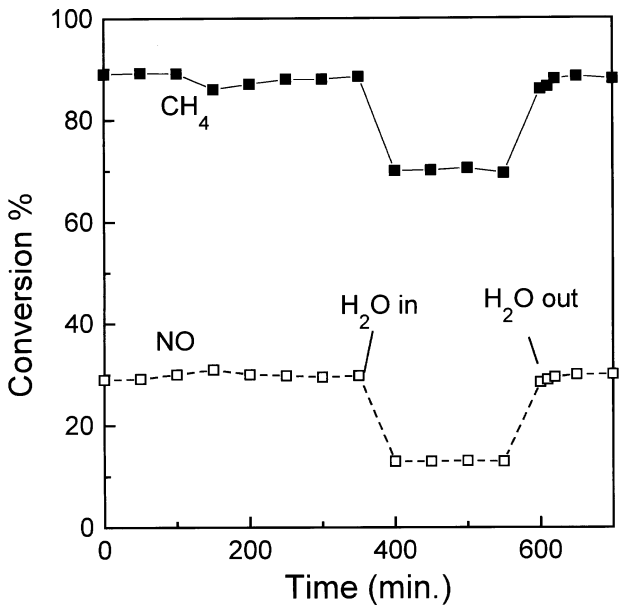

Figure 3. Effect of the water addition (3%) on the: (○) NO_x to N_2 conversion and (■) CH_4 to CO_x conversion. Reaction conditions see figure 2.

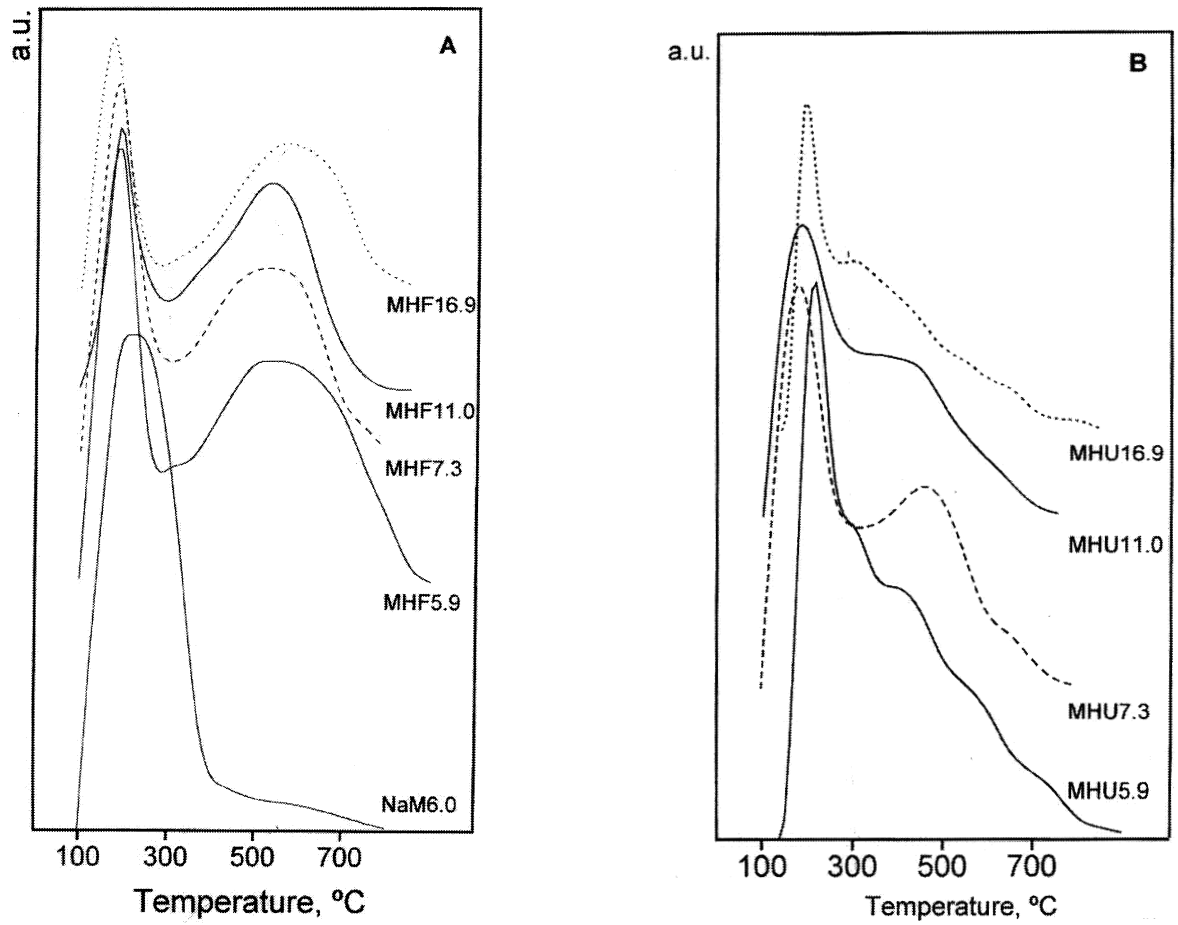

Figure 4. TPD of NH_3. Heating rate 10°C min^{-1}. Final temperature: 700°C, kept constant till the end of desorption. (A) Fresh samples. (B) After 1 h on stream at 650°C.

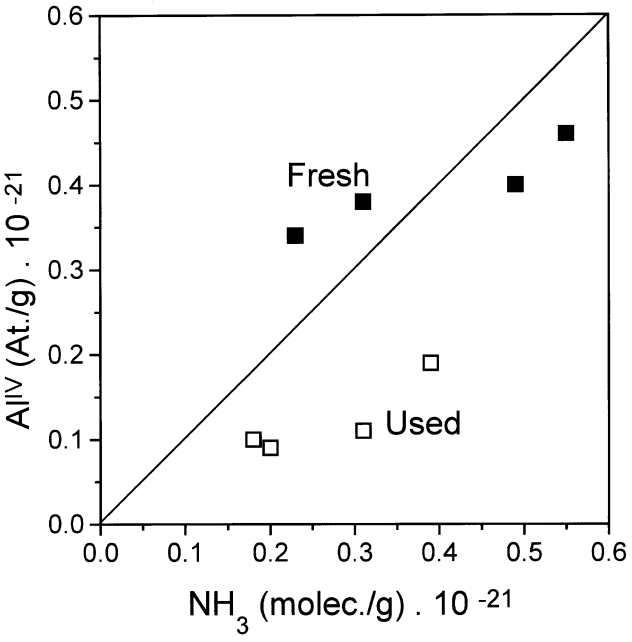

Figure 5. Correlation between concentration of Al^{IV} determined by ^{27}Al MAS NMR and strong acid sites (NH_3 TPD from table 1 second peak). (■) Fresh samples. (□) Used samples. The diagonal corresponds to $NH_3 2P/Al^{IV} = 1$.

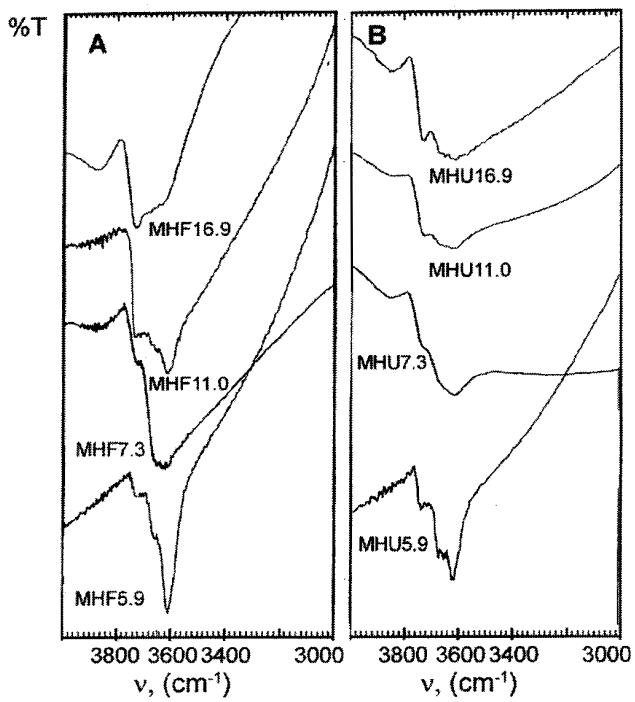

Figure 6. Effect of increasing dealumination upon the hydroxyl band intensities of H-mordenites. (A) Fresh samples. (B) Used samples.

1 h on stream at 650°C) on the acidic properties of the samples studied. The maxima corresponding to the strong acid sites are less defined and shifted to lower temperatures while the amount of desorbed NH_3 is lower than that in the fresh samples (table 1, figure 5). This would suggest either a redistribution of the acid sites or a blocking of the zeolite pores by amorphous aluminium which could restrict the accessibility of acid sites to NH_3 molecules.

Additional information on Brønsted sites was obtained by analyzing the fresh and used samples through FTIR in the 3600 to 3800 cm^{-1} region. The results obtained are shown in figures 6A and 6B. The solid with a lesser degree of dealumination, fresh MH5.9 (figure 6A), presents three well-defined bands which in decreasing intensity order are the following: 3608, 3657 and 3732 cm^{-1}. The band at 3600 cm^{-1} is associated with the vibrations of the OH groups linked to the Brønsted sites (Si–OH–Al), while the signal at 3657 cm^{-1} is assigned to the OH linked to the extra-lattice Al and the band at 3732 cm^{-1} is related with the Si–OH groups appearing as a consequence of dealumination, which are associated with the defects in structure or with amorphous silica [20–22].

As the dealumination by acid treatment progresses and the Si/Al ratio increases, it can be observed that the intensity of the band at 3608 cm^{-1} decreases. The intensities of the bands at 3657 and 3732 cm^{-1} become important in the samples with less Al content in the lattice, particularly the silanol group band.

The spectra obtained with the used samples (figure 6B) are in general comparable to those of the fresh samples but with less defined signals. This type of broadening was also observed by Ha et al. [23] in their studies on the effect of thermal treatments with different degrees of humidity on the dealumination of H-mordenites.

3.3. ^{129}Xe NMR of physisorbed xenon

The extra-lattice aluminum species which appear as a consequence of the dealumination suffered by the solid under reaction conditions (table 1) could be located either in the main channel or obstructing the access to the side-pockets and, consequently, they could impair the free diffusion of the NH_3 molecules to the acid sites. In an attempt to throw light on such process, ^{129}Xe NMR experiments were performed on fresh and used samples. The spectra of physisorbed xenon for the MH5.9 fresh and used samples are shown in figure 7 for a pressure of approximately 200 mbar and 20°C. The spectrum corresponding to the Na-mordenite sample is also shown as a reference. The MH5.9 shows a single peak due to the well-known coalescence effect, indicating the xenon free exchange between the main channels and the side-pockets. However, after the catalysts have been on stream for 1 h at 650°C, the peak corresponding to the side-pockets starts appearing again, even though smaller if compared to the Na-mordenite. These results suggest that the non-framework Al species formed under reaction conditions at high temperatures, viz. 650°C, may obstruct the access to the mordenite side-pockets as

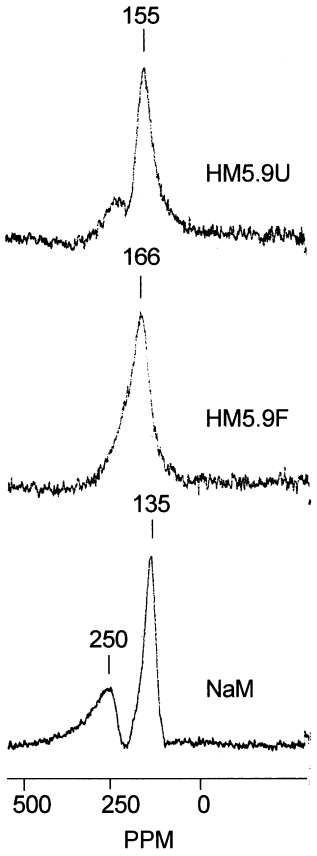

Figure 7. ^{129}Xe NMR of physisorbed xenon (at 20°C) on fresh and used MH5.9 as compared with Na-mordenite.

Na does. Comparable results were obtained with samples with different Si/Al ratios.

When the chemical shift (ppm) of the main peak is plotted against the amount of adsorbed xenon (figure 8), it also suggests the presence of extra framework Al species in the main channels of the mordenite structure [24]. Compare fresh and used MH5.9 with the Na-mordenite reference sample.

The amorphous extra-lattice Al species that already exist in the acid-treated H-mordenite may be located in the main channels as suggested by the ^{129}Xe NMR data (figures 7 and 8) but they cause a minor blocking of the side-pockets (figure 7). In the used samples, such species and the ones formed during reaction would migrate as a consequence of the reaction atmosphere obstructing the access to the side-pockets as revealed by the ^{129}Xe NMR spectra (figure 7). Further results shown in figure 8 are indicative of a large amount of non-structural Al inside the channels if the used samples are compared to the fresh ones. These results suggest that pore blocking is the main cause for the apparent change in the distribution of the acid strength observed in the used H-mordenites (figure 4B). This coincides with one of the explanations given by Miller et al. [24] to account for the changes they observed in their TPD profiles after thermal treatment at 750°C for 8 h.

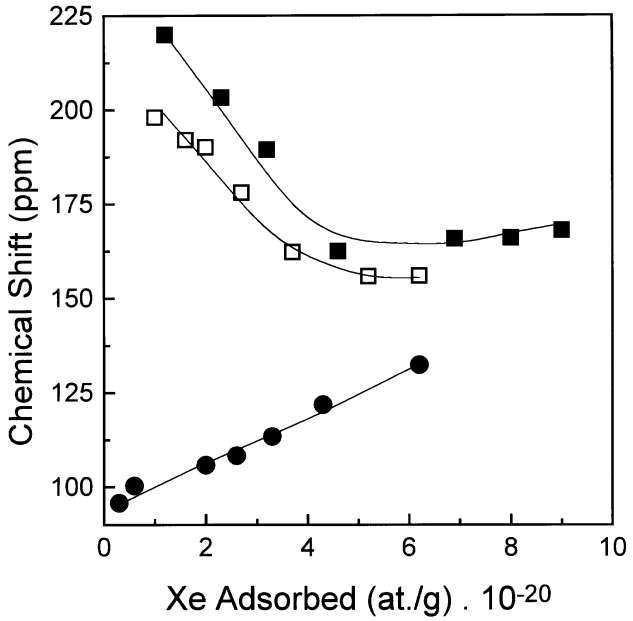

Figure 8. ^{129}Xe chemical shift at different concentrations of adsorbed xenon on: (■) MH5.9 fresh catalyst, (□) MH5.9 used catalyst, (●) Na-mordenite.

3.4. Kinetic parameters

To obtain the kinetic parameters the flow reactor was operated under differential conditions. Both fresh and deactivated catalysts were used in these studies. The rates of reaction were obtained in a temperature range of 450 to 550°C and at space velocities (GHSV) of 6,500 to 60,000 h^{-1}. It was verified that both the NO and CH_4 conversions showed a linear dependency with the inverse of the space velocity. In all cases, the conversion was limited to below 10%.

Alternatively working with constant methane, NO and oxygen concentrations, the reaction orders at 450, 500, 525 and 550°C were obtained from logarithmic plots; they are shown in table 2. The orders with respect to oxygen were near zero in all cases. Figure 9 shows the Arrhenius plot for the rates of methane combustion and NO conversion to N_2. Note that the activation energies for both reactions are almost the same. Moreover fresh and used catalysts also yield the same value.

In recent publications, Li and Armor [25], Cowan et al. [26], and Lukyanov et al. [13] performed kinetic studies for the SCR of NO_x with CH_4 on Co-ferrierite (the first authors) and Co-ZSM5 (the other ones). The kinetic orders reported in the three studies are practically coincident, varying with the reaction temperature. As far as we know, no reaction orders for H-zeolites have been reported in the literature. The reaction orders for H-mordenite (table 2) are higher than those reported for Co-zeolites. This difference is more pronounced in the case of NO and may be a result of the nature of the exchanged cations.

Table 2
Empirical reaction orders

Temperature (°C)	Reaction orders [a]					
	a	*b*	*c*	*d*	*e*	*f*
			fresh catalyst			
450	0.43	0.65	0.03	0.85	0.26	0.04
500	0.68	0.97	0.02	0.97	0.43	0.04
525	0.60	0.91	0.01	1.16	0.51	0.08
550	0.66	0.87	0.01	1.40	0.47	0.02
			used catalyst			
	0.71	0.47	0.02	1.37	0.25	0.02

[a] *a*, *b*, *c*, *d*, *e* and *f* are the empirical reaction orders of the following kinetic equations: $d[NO]/dt = -k_1[NO]^a[CH_4]^b[O_2]^c$; $d[CH_4]/dt = -k_2[NO]^d[CH_4]^e[O_2]^f$.

Our activation energies are practically coincident with those reported by Lukyanov et al. [13] for H-ZSM5. Unfortunately, these authors did not report kinetic orders for this catalyst. In their work, they verified that the kinetic parameters obtained under differential conditions were also valid in the integral regime. In the present work, we performed a similar test, numerically integrating the kinetic expressions (see experimental section). Figure 10 shows an excellent agreement between the experimental values obtained at different space velocities and the concentration values calculated with the kinetic parameters obtained under differential conditions at 550°C.

In the kinetic data here reported, the difference observed in the orders with respect to NO stands out. The orders are higher in the H-mordenite than in Co-zeolites [13,25,26]. This may be explained by the observed differences in the adsorbed species seen using FTIR on Co- and H-mordenites. Imoberdorf et al. [27] found that the former shows larger amounts of adsorbed NO and lower temperatures for NO_2 formation than H-mordenites.

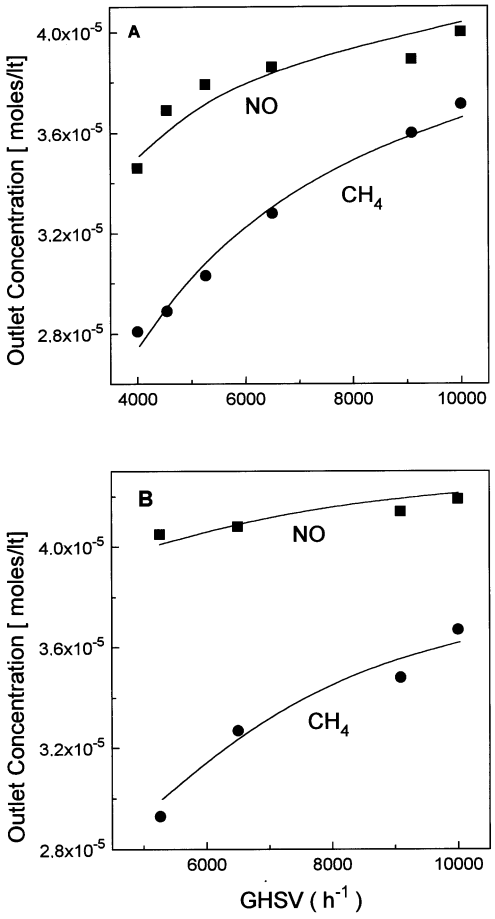

Figure 10. Comparison of experimental (points) and simulated (curves) outlet reactor concentrations during the SCR reaction over MH5.9 at 550°C. The solid lines were obtained by numerical integration of eqs. (2) and (3). (A) Fresh samples. (B) Used samples.

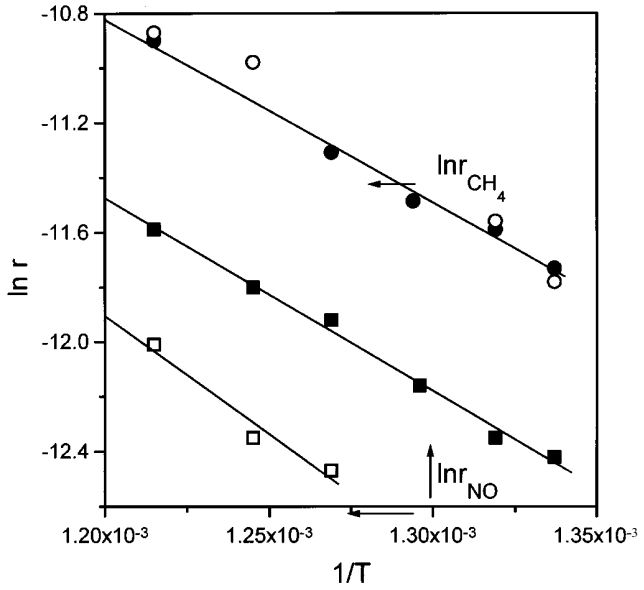

Figure 9. Arrhenius plots for the rates of NO conversion to N_2 (r_{NO}) and CH_4 combustion (r_{CH_4}). Solid symbols: fresh catalyst. Open symbols: used catalyst.

An interesting aspect of the present work is that the activation energies obtained with fresh and used (partially deactivated) catalysts are coincident. It is then concluded that the lower activity observed in the catalysts subjected to reaction temperatures higher than 650°C is fundamentally due to a decrease in the pre-exponential factor. This is consistent with a decrease concentration of active sites in the used samples or pore blockage due to dealumination.

3.5. Catalytic acitivity and acid sites

In an attempt to correlate the activity of H-mordenite for the SCR of NO_x with CH_4 with their acid properties, the rate of NO disappearance over the different solids studied was plotted against the number of NH_3 mole-

cules desorbed at high temperature (figure 11). The linear correlation obtained with the fresh samples would suggest that the activity for NO to N_2 conversion depends on the strong acid site concentration on H-mordenites. In our study [17] of the role of the different aluminum species on the SCR of NO with methane on H-mordenite, we concluded that the active site for such reaction was related to framework Al^{IV}. Murakami and coworkers [11] in their studies of the SCR of NO with C_3H_6 over various H-form and ion exchanged zeolites, including H-mordenites with different Si/Al ratios, reported that the activity of NO reduction increased proportionally to the acid site concentration. However, they found that H-mordenite was the exception to this behavior. Murakami and coworkers argue that such discrepancy could be attributed to the carbonaceous materials that were formed under their reaction conditions.

Both straight lines, obtained with fresh and used samples, are parallel with the latter shifted to lower amounts of desorbed NH_3 molecules (figure 11). This would first confirm that in used samples some of the strong acid sites might not be accessible to the NH_3 molecule, due to the blocking of the pores (vide supra). However, such sites may act as active sites for the reaction as was previously reported [17].

The results shown in figure 12, where selectivity is plotted against NH_3 desorbed at high temperature, suggest that acid sites play no important role in those steps defining N_2 selectivity in the SCR of NO_x. These results are consistent with the hypothesis of the common intermediate in the oxidation of CH_4 with NO_x or oxygen as proposed by several authors [13,26].

4. Conclusions

Our results show that:

(i) The rate of NO disappearance correlates with the concentration of strong acid sites in H-mordenites (figure 11).

(ii) These acid sites are not a major factor in determining the selectivity (NO conversion/CH_4 conversion) of the reduction of NO_x with CH_4 (figure 12).

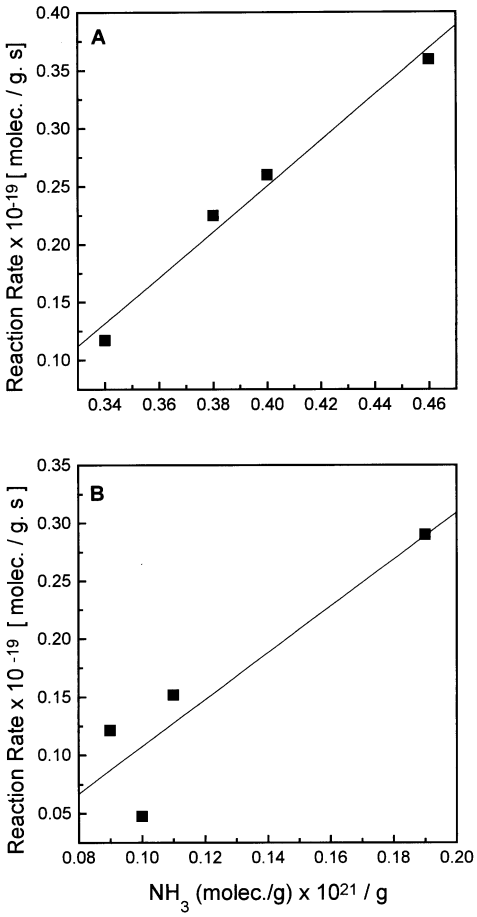

Figure 11. Effect of acid sites concentration (NH_3 TPD from table 1 second peak) upon NO dissappearance rate. (A) Fresh samples. (B) Used samples. Reaction conditions: GHSV: 6500 h^{-1}, temperature: 525°C, NO: 1000 ppm, CH_4: 1000 ppm, O_2: 10%, the balance to one atmosphere with He.

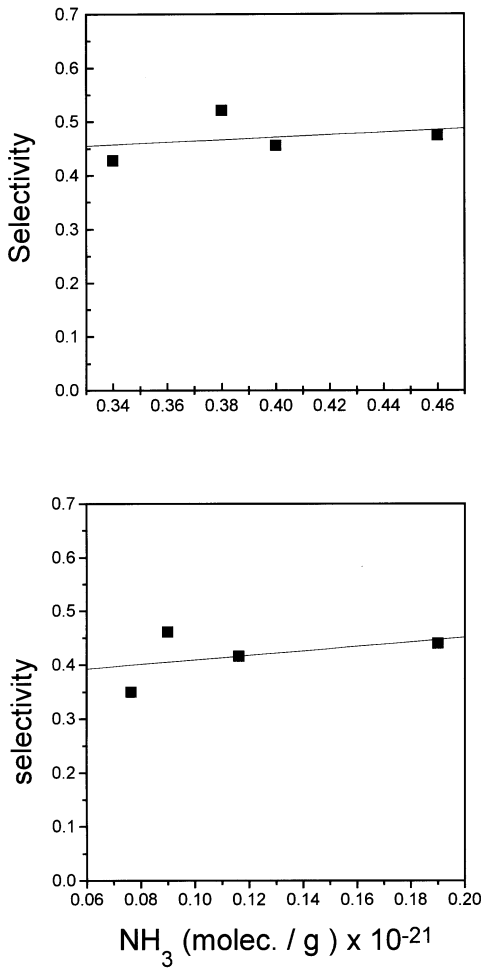

Figure 12. The selectivity is not affected by acid sites concentration. Selectivity is defined as NO conversion/CO conversion. Reaction conditions given in figure 11.

(iii) H-mordenites after being on stream for 1 h at 650°C suffer a dealumination process and consequently a decrease of the strong acid sites concentration, that produces a decrease of the activity of the solids (table 1).

(iv) Comparable reaction orders and the same activation energies for fresh and deactivated H-mordenites are consistent with the view that the deactivation process is originated in a decrease in the number of active sites but not in a change in nature.

(v) The similar activation energies obtained for the NO reduction in N_2 and CH_4 oxidation in CO_x would agree with the concept proposed by Hall and coworkers that these two reactions are coupled and have the same rate-limiting step [13].

(vi) ^{129}Xe NMR confirms that both pre-existing extra-lattice aluminum and those produced on stream migrate at $T > 650$°C in the reacting environment. These aluminum-containing moieties partially obstruct the Xe free exchange between the main channels and the side pockets (figures 7 and 8).

(vii) The NH_3 TPD might be unable to count the total acid sites in the deactivated H-mordenite that could act as active site on the SCR of NO_x with CH_4 due to pore-blockage (figures 4B, 7 and 8).

Acknowledgement

This work was performed under European Union Contract # C11*CT93-0090. The authors are indebted to Conicet and UNL for their partial support and to the Japan International Cooperation Agency for the donation of the IR spectrometer to the National Catalysis Center. The authors also thank Elsa Grimaldi for her help in the edition of the English manuscript.

References

[1] Y. Li and J.N. Armor, Appl. Catal. B 1 (1992) 131.
[2] J.N. Armor, Catal. Today 26 (1995) 147.
[3] Y. Li and J.N. Armor, J. Catal. 150 (1994) 376.
[4] Y. Li and J.N. Armor, J. Catal. 150 (1994) 388.
[5] Y. Li and J.N. Armor, J. Catal. 145 (1994) 1.
[6] Y. Mishizaka and M. Misono, Chem. Lett. (1993) 2237.
[7] C.J. Loughram and D.E. Resasco, Appl. Catal. B 7 (1995) 113.
[8] K. Yogo, M. Umeno, H. Watanabe and E. Kikuchi, Catal. Lett. 19 (1993) 131.
[9] Y. Kintaichi, H. Hamada, M. Tabata, M. Sasaki and T. Ito, Catal. Lett. 6 (1991) 239.
[10] H. Hamada, Y. Kintaichi, M. Tabata, M. Sasaki and T. Ito, Chem. Lett. (1991) 2179.
[11] A. Satsuma, K. Yamada, T. Mori, M. Niwa, T. Hattori and Y. Murakami, Catal. Lett. 31 (1995) 367.
[12] D.B. Lukyanov, G. Sill, J. d'Itri and W.K. Hall, J. Catal. 153 (1995) 265.
[13] D.B. Lukyanov, E.A. Lombardo, G. Sill, J.L. d'Itri and W.K. Hall, J. Catal. 163 (1996) 447.
[14] R.A. Grinsted, H.W. Zhen, C. Montreuil, M.J. Rokosz and M. Shelef, Zeolites 13 (1993) 602.
[15] J.N. Armor and T.S. Farris, Appl. Catal. B 4 (1994) L11.
[16] J.Y. Yan, G.D. Lei, W.M.H. Sachtler and H.H. Kung, J. Catal. 161 (1996) 43.
[17] M. Lezcano, A. Ribotta, E. Miró, E. Lombardo, J. Petunchi, C. Moreaux and J.M. Dereppe, J. Catal. 168 (1997).
[18] B.L. Meyers, T.H. Fleisch, G.J. Ray, J.T. Miller and J.B. Hall. J. Catal. 110 (1988) 82.
[19] M. Lezcano, A. Ribotta, E. Miró, E. Lombardo, J. Petunchi, C. Moreaux and J.M. Dereppe, in: *Studies in Surface Science and Catalysis*, Vol. 101 B (Elsevier, Amsterdam, 1996) p. 971.
[20] J. Rocha and J. Klinowski, Synthesis of Microporous Materials 1 (1992) 70.
[21] M. Sawa, M. Niwa and Y. Murakami, Zeolites 10 (1990) 532.
[22] G.R. Hays, W.A. Van Erp, N.C.M. Alma, P.A. Couperuf, R. Huis and A.E. Wilson, Zeolites 4 (1984) 373.
[23] B.B. Ha, J. Guibet and D. Barthomeuf, J. Chem. Soc. Faraday Trans. I 75 (1979) 1245.
[24] J.T. Miller, D.D. Hopkins, B.L. Meyers, G.J. Ray, R.T. Roginsky, G.W. Zajac and Rosenbaum, J. Catal. 138 (1992) 115.
[25] Y. Li and J. Armor, J. Catal. 150 (1994) 376.
[26] A. Cowan, R. Dümpelmaun and N. Cant, J. Catal. 151 (1995) 356.
[27] G. Imoberdorf, M. Kurgansky, M. Ulla, E. Miró and J. Petunchi, to be published.